C.2

SERI/TP-32-252

SERI/TP-32-252
UC CATEGORY: UC-63E

PROPERTY OF
U. S. GOVERNMENT

SOLAR ENERGY RESEARCH INSTITUTE
Solar Energy Information Center

JUL 30 1979

GOLDEN, COLORADO 80401

EVIDENCE FOR THE SEGREGATION OF IMPURITIES TO GRAIN BOUNDARIES IN MULTIGRAINED SILICON USING AES AND SIMS

L. L. KAZMERSKI
P. J. IRELAND
T. F. CISZEK

TO BE PUBLISHED IN JOURNAL OF APPLIED PHYSICS.

Solar Energy Research Institute

1536 Cole Boulevard
Golden, Colorado 80401

A Division of Midwest Research Institute

Prepared for the
U.S. Department of Energy
Contract No. EG·77·C·01·4042

ABSTRACT

The first direct physical evidence is presented for the segregation of impurities to grain boundary regions in cast and directionally solidified multigrained silicon. Complementary scanning Auger microprobe (SAM) and secondary ion mass spectroscopy (SIMS) techniques are used in conjunction with in-situ ultrahigh vacuum fracturing of the multigrained silicon to identify impurities and their localization at the grain boundaries. Both grain and grain boundary regions are exposed for comparative examination under identical experimental conditions. Auger mapping methods are used to show impurity distributions (including Ni, Al, C and O) at grain boundaries. SIMS provides information on trace impurities that are below the detectability limits of Auger electron spectroscopy (AES). The impurities, which include C, Cr, Fe, Co, Zn, Cu, Al, Ni, Sb, Ti and Mg, depend upon the growth technique and containing crucible as well as the silicon source material.

I. INTRODUCTION

Among the major impediments to the large-scale deployment of photovoltaic cells is the high cost of semiconductor material. This is especially evident in the case of the single-crystal silicon solar cell, which has demonstrated its effectiveness and reliability for space applications and is the only solar cell commercially available for specialized terrestrial use. However, its cost is a complex function of energy-intensive fabrication processes, the high cost of material and single crystal production, and the material-consumptive wafer cutting and preparation procedures.[1] Alternatives to the single-crystal silicon converter are under investigation, including long-range options for intermediate efficiency thin-film and very high efficiency concentrator photovoltaic devices.[2,3] Because of material availability and the large scientific database compiled for this semiconductor, silicon remains attractive for photovoltaics. Attempts at using polycrystalline, thin-film silicon for solar cells have generally provided devices with less adequate performance dominated by grain boundary recombination mechanisms.[4,5] Recently, however, devices with efficiencies approaching those of single-crystal types have been reported for cells fabricated from large-grain (1-10 mm diameter) silicon grown by a casting technique.[6-8] A micrograph of a typical sample is shown in Fig. 1. This multigrained or semicrystalline material has both cost and energy saving potential compared to Czochralski or float-zone counterparts. Another important factor, which forms the basis for this paper, is that the casting process seems to foster the migration of impurities - which may originate in the silicon source material or be extracted from the crucible that contains and shapes the ingot - to the grain boundary regions. This localization of impurities has important implications for both improving multigrained solar cell performance by passivating the grain boundaries and for reducing device costs by perhaps allowing the use of lower purity starting material.

This paper presents the first direct physical evidence for the localization of impurities at the grain boundary regions in silicon grown by the casting and related directional solidification techniques. Complementary scanning Auger microprobe (SAM) and secondary ion mass spectroscopy (SIMS) techniques are used in conjunction with <u>in-situ</u>, ultrahigh vacuum fracturing of the multigrained silicon to identify and examine the segregation of impurities resulting from the growth processes. By these procedures, both grain and grain boundary regions are exposed for comparative examination under identical experimental conditions.

II. EXPERIMENTAL PROCEDURES

The multigrained silicon samples used in this study were obtained from three sources. Two of them (termed Si-A and Si-B in this paper) were produced by a "conventional" casting process in which the silicon was molten when it was poured into a shaping crucible held slightly below the melting point of the silicon.[9] The third sample type (termed Si-C) was produced by the directional solidification process.[10] This differs from casting in that solid silicon was loaded into the crucible and then heated into the molten phase. In either case, the cooling and cooling rates were precisely controlled to provide optimal grain size and structure. Both carbon and Al_2O_3-based crucibles were used to form the multigrained silicon ingots which were then sliced into thin (<1 mm thick) sheets.

The surface analytical operations were performed in a Physical Electronics Industries Model 590 scanning Auger microprobe system with secondary ion mass spectroscopy capabilities. The minimum beam diameter of the SAM was measured to be 1600Å. A differentially pumped argon ion gun was used for depth profiling and SIMS. Its beam diameter could be focused to 140 μm. The base pressure of the analysis chamber was 1.2×10^{-10} torr. An Extranuclear Laboratories quadrupole mass analyzer was used for the SIMS, and elemental and molecular species of 1 to 1000 AMU could be analyzed. The samples were inserted using an introduction/transfer system which preserved the UHV chamber conditions, minimizing contamination to the volume. A sample fracture stage permitted the in-situ ultrahigh vacuum exposure and comparison of both intragrain and grain boundary regions. The condition of the fracture (i.e., whether through a grain or along a grain boundary) was verified by comparing the topographies and impurity contents to those of control samples fractured outside the analysis chamber. These control samples were etched slightly in a weak NaOH solution in order to better delineate the grain boundary intersections with the sample surface. With sufficient care, the fracture could be confined to a desired region, and the location of the fracture (i.e., whether through a grain, along a boundary, or some combination) could be ascertained by comparison with the original condition as recorded by an optical micrograph. A typical fracture region is shown in the secondary electron micrograph of Fig. 2. Through experience with the fracturing process, the smooth portion [labeled (a)] is determined to be a grain boundary area. Fractures through the grain itself [labeled (b)] were generally more structured. In most cases this desirable side-by-side analysis situation was provided by the fracturing procedure. By the UHV fracturing technique, potential contamination

to these surfaces from sorbed species was minimized, thus ensuring that the resulting data were not artifacts of the experiment. The chamber environment was monitored during the experiment with a separate quadrupole mass analyzer with residual gas analysis capability.

III. RESULTS AND DISCUSSION

This investigation involves the application of two surface analysis techniques, SAM and SIMS, to the solution of the impurity segregation problem. Since each contributes its inherent diagnostic quality (e.g., submicron spatial resolution, nondestructive analysis, monolayer surface sensitivity, quantifiable data, and nearly uniform elemental sensitivity for SAM; increased sensitivity, usually 100 times better than Auger, isotope and molecular fragment identification for SIMS), the methods are complementary. Thus, they provide far more dependable and less ambiguous results if used, as in this study, for essentially simultaneous analysis during the diagnostic procedure.

A. Auger Studies

Initial attempts were made to analyze the composition of the grain boundary regions in the multigrained silicon wafer as it is normally prepared for device fabrication. In this configuration, the grain boundaries are readily recognizable (see Fig. 1) but offer a low surface area for analysis since they run practically perpendicular to the exposed surface. Even with minimal electron beam diameter, analyses using this configuration proved to be nonreproducible and inconsistent, although it does give an indication of the impurity localization effects. Thus, the in-situ fracturing of the samples is utilized to provide increased analysis areas (see Fig. 2). Two benefits are realized using this technique: (1) since the fracturing and exposure is accomplished under UHV conditions, the probability of generating external impurity artifacts on the analysis area through handling is minimized; and, (2) the fracturing, as observed in Fig. 2, can provide exposure of both grain and grain boundary regions for side-by-side analysis.

Fig. 3 shows an Auger point analysis of both the grain (a) and grain boundary (b) for a Si-C (directionally solidified) sample. These data were taken in a region near the center of the wafer, approximately 2 cm from the crucible wall, with a 1.0 μm beam size for analysis. The Auger spectrum for the grain regions shows the presence of only Si and the intentional dopant, B. However, the identical scan of the boundary indicates the presence of B, C, Fe, Si and SiO_x. This sample was solidified in a carbon crucible which is the origin of the carbon in the Auger spectra. The carbon levels were noticeably higher in the grain boundaries examined near the outer edge of the 5 cm wafer. Near the perimeter, carbon inclusions were detected in some of the grains themselves, but very few such inclusions were observed in the central regions. This is consistent with the expected higher carbon content in the liquid near the dissolution boundary. The Fe,

which was detected on all boundary regions analyzed, is assumed to originate in the Si source material since no Fe was detected in the carbon crucible material. The Si-starting material was not available for analysis. The Fe concentration levels were fairly consistent from the center of the wafer to the outer edge, with concentrations as high as the 1 atomic-% level at the grain boundaries. If any impurities existed in the grains, they were below the detectability limits (~0.1 atomic-%) of Auger electron spectroscopy.[11]

An Auger mapping of a grain boundary area is presented in Fig. 4. These data were taken on an internal region of cast sample Si-A grown in a ceramic crucible. The secondary electron image of the fractured grain boundary region does show some irregularities as indicated at points 1 and 2. The Auger maps of this region do give evidence of impurity concentrations (Ni, Al and C) in these areas with oxygen prevalent throughout. It should be emphasized that the Auger maps here indicate buildup of the impurities which can be remnants due to fracturing, and lower concentrations of each are detectable throughout the grain boundary regions. No impurities were found in the grain interiors. The grain boundary localization of the Ni and Al (in the form of NiO and Al_2O_3, probably from the crucible) is verified in the depth-compositional profile of Fig. 5 and corresponds to point 2 of Fig. 4. These data show that the Al, Ni and O concentrations diminish as the grain region, shown by the increase of the Si signal, is reached. It is also evident that the Al_2O_3 and NiO occur in alternating higher concentration layers perpendicular to the grain. These data are not caused by sputter-crater edge effects [12, 13] since the sputter beam was rastered over a 1 mm by 1 mm area while the Auger electron analysis beam was only some 1600Å in diameter. Other impurities, both in this and other multigrained samples, showed similar grain boundary localization evidenced by the depth-profiling techniques.

These Auger electron spectroscopy data are presented as examples of the localization evidence. Cast samples (Si-A and Si-B) and the directionally solidified samples (Si-C) showed similar results. Only the elemental impurities, due to the difference in crucible and starting materials, differed between sample types. Essentially no unintentional impurities, outside of the C inclusions for sample Si-C, were detected in the interior of the grains. Since the Auger technique is insensitive to concentrations at or below the 10^{18}-$10^{19}/cm^3$ level, the determination of trace impurity content necessitated the use of another surface-sensitive method.

B. SIMS Studies

Generally, SIMS provides at least 100 times the sensitivity to trace elements of that attainable by Auger spectroscopy.[14] It is, however, limited in spatial resolution by the broader diameters (usually greater than 100 μm) of the ion probes. In the configuration for these experiments, SIMS can be performed on the same region as the SAM investigations without moving or otherwise disturbing the sample itself.

The analysis once again could be performed on adjacent grain and grain boundary fractured regions, as shown in Fig. 2. Fig. 6 presents a typical SIMS spectrum for a region formed by fracturing through a grain, this time from sample Si-A. A controlled oxygen leak (10^{-7} torr) is used to enhance secondary ion yields. The SIMS spectrum indicates primarily the presence of Si; the only impurity is the intentional dopant. The oxides result from the oxygen leak, and the Na and K result from the inevitable inclusion of the top and/or bottom surfaces of thin samples (previously exposed to the atmosphere) in the SIMS analysis. In contrast, many impurities are observed in fractures at the grain boundary (see Fig. 7). These data are taken on the identical region presented in the Auger studies of Figs. 3 and 4. In addition to the C, Ni and Al, trace impurities including Ti, Cu, B and Mg are detected. None of them appear in the corresponding analysis performed on the grain region. SIMS profiles do confirm that the impurities are localized at the boundary and do not significantly penetrate the grain itself. Figs. 8 and 9 present similar SIMS data taken on the cast Si-B and directionally solidified Si-C multigrained samples. In similarly fashion, the grains were relatively free of impurities and localization occurred at the boundaries. Results of a bulk analysis performed independently on sample Si-B indicate the presence of all the impurities detected in the SIMS analysis of Fig. 8. From this bulk analysis, average concentrations (except for C, O, B and Si) are generally in the 10^{11}-$10^{14}/cm^3$ range, which seems to correlate with that detectable by the SIMS method if they were indeed confined primarily to the grain boundary regions.

The distribution of impurities as detected by SIMS is not uniform throughout all samples. Nor is it uniform in all grain boundaries of a given sample. Fig. 10 illustrates such a difference. These data are taken on a grain boundary in the same region as that shown in Fig. 7 (approximately 3 mm away). The SIMS spectrum, taken under the identical experimental conditions used to generate the data of Fig. 7, shows some differences, notably the lack of the Mg, Cu, Ti and Ni peaks. The reasons for these differences can only be speculated upon and need further investigation to provide any conclusions. However, these differences might correlate with previous reports that not

all grain boundaries exhibit the same electrical behavior.[6] Experiments are underway in this laboratory to correlate grain boundary electrical activity and impurity composition.

IV. SUMMARY AND CONCLUSIONS

A summary of the Auger electron spectroscopy and SIMS investigations comparing the impurity content detected in the grain and grain boundary regions of the multigrained silicon is presented in Table I. This paper presents the first direct physical evidence for the segregation and localization of such impurities at grain boundaries in both cast and directionally solidified samples. Although the impurity level and content of the grain boundaries seem to differ even in the same sample, the grains themselves appear relatively free from such impurities, at least within the detectibility limits of the surface analysis techniques employed. Further work is needed to correlate the results of this investigation with probable effects of impurity content on the electrical behavior of the grain boundaries.

Acknowledgement

The authors sincerely appreciate the valuable criticisms and discussions of Dr. Sigurd Wagner, SERI, in the evolution of this manuscript. The authors also thank Ms. Joyce Barrett for her editorial help with this paper.

REFERENCES

1. R. G. Forney, in Proceedings of the Semiannual Review Meeting, Silicon Technology Programs (Department of Energy, Washington, DC; 1978) pp. 95-155.

   Also, P. D. Maycock, Proceedings of the 13th IEEE Photovoltaic Spec. Conf.— Washington, DC (IEEE, New York; 1978) pp. 5-8.

2. H. Ehrenreich, Ed. American Physical Society Study on Solar Photovoltaic Energy Conversion (American Physical Society, New York; 1979)

3. E. A. DeMeo and P. B. Bos, Perspectives on Utility Central Station Photovoltaic Applications, EPRI Rpt. ER-589-SR (Electric Power Research Institute, Palo Alto, CA; 1978).

4. T. L. Chu, S. S. Chu, C. L. Lin and R. Abderrassoul, J. Appl. Phys. 50, 919 (1979).

5. C. H. Seager and D. S. Ginley, Appl. Phys. Lett. 34, 337 (1970).

6. J. Lindmayer, Proceedings of the 13th IEEE Photovoltaics Spec. Conf. - Washington, DC (IEEE, New York; 1978) pp. 1096-1099.

7. J. Lindmayer, Proceedings of the 12th IEEE Photovoltaics Spec. Conf. - Baton Rouge, LA (IEEE, New York; 1976) pp. 82-85.

8. H. Fisher and W. Pschunder,Proceedings of the 12th IEEE Photovoltaics Spec. Conf. - Baton Rouge, LA (IEEE, New York; 1976) pp. 86-92.

9. R. F. Bunshah, in Techniques of Metals Research: Materials Preparation and Handling, Part 2 (John Wiley, New York; 1968) pp. 775-832.

10. T. F. Ciszek, G. H. Schwuttke and K. H. Yang, J. Cryst. Growth 46, 527 (1979).

11. L. E. Davis, N. C. MacDonald, P. W. Palmberg, G. E. Riach and R. E. Weber, Handbook of Auger Electron Spectroscopy (Physical Electronics Industries, Inc., Eden Prairie, Minnesota; 1976) pp. 1-18.

12. J. M. Morabito and P. M. Hall, Proceedings 9th Annual Scanning Electron Microscopy Symposium, Chicago, IL (ITT Press, Chicago, 1976) pp. 221-230.

13. J. M. Morabito and R. K. Lewis, in Methods of Surface Analysis (Elsevier Scientific Pub. Co., New York; 1975) pp. 279-328.

14. J. A. McHugh, in Methods of Surface Analysis (Elsevier Scientific Pub. Co., New York; 1975) pp. 223-278.

TABLE I. **Summary comparison of impurity content of multigrained Si samples fractured in ultrahigh vacuum. (O) indicates that the data were taken with an oxygen leak to enhance secondary ion yields.**

		Si-A	Si-B	Si-C
AES	Grain	Si	Si	Si
		P		B
	Grain Boundary	SiO_x, Si	SiO_x, Si	SiO_x, Si
		C	C	C
		Ni	Ni	Fe
		Al		
SIMS	Grain	Si	Si	Si
		P	B	B
				C
	Grain Boundary	SiO_x	SiO_x	SiO_x
		Al (O)	C	Al (O)
		Ni (O)	B	C
		Ti (O)	Zn (O)	Fe (O)
		B	Cu (O)	B
		Cu (O)	Ni (O)	
		Mg (O)	Cr (O)	
			Fe (O)	
			Sb (O)	
			Co (O)	
			Al	

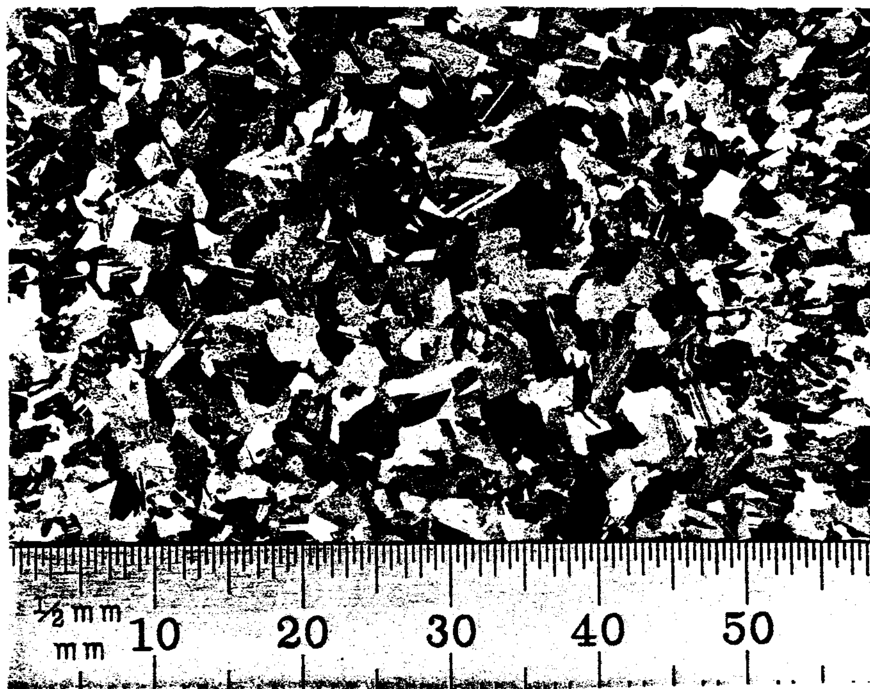

Fig. 1 Micrograph of multigrained silicon sample.

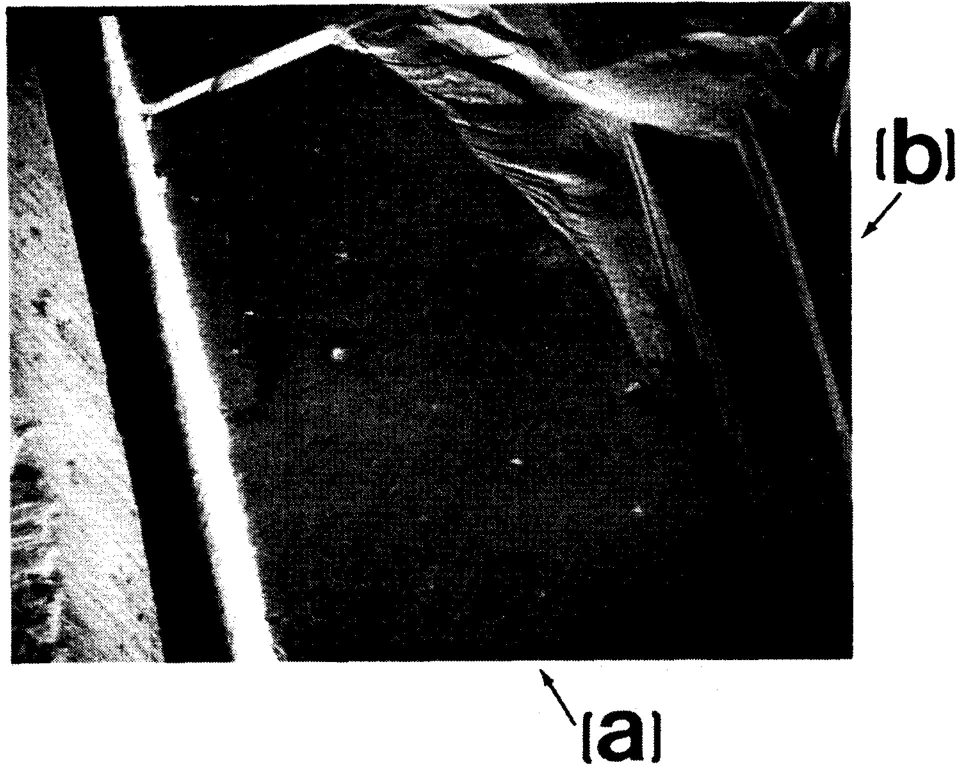

Fig. 2 Secondary electron detection image of fractured multigrained silicon: (a) Grain boundary region; (b) Grain region.

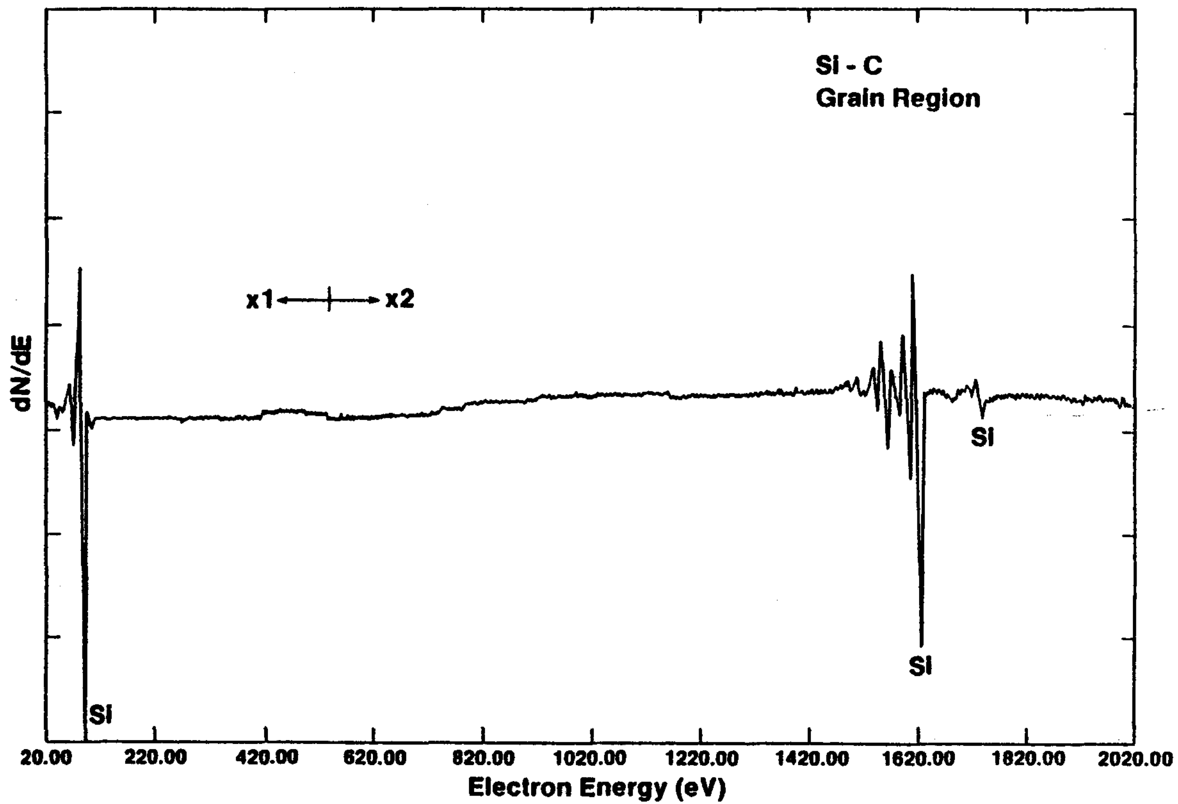

(a)

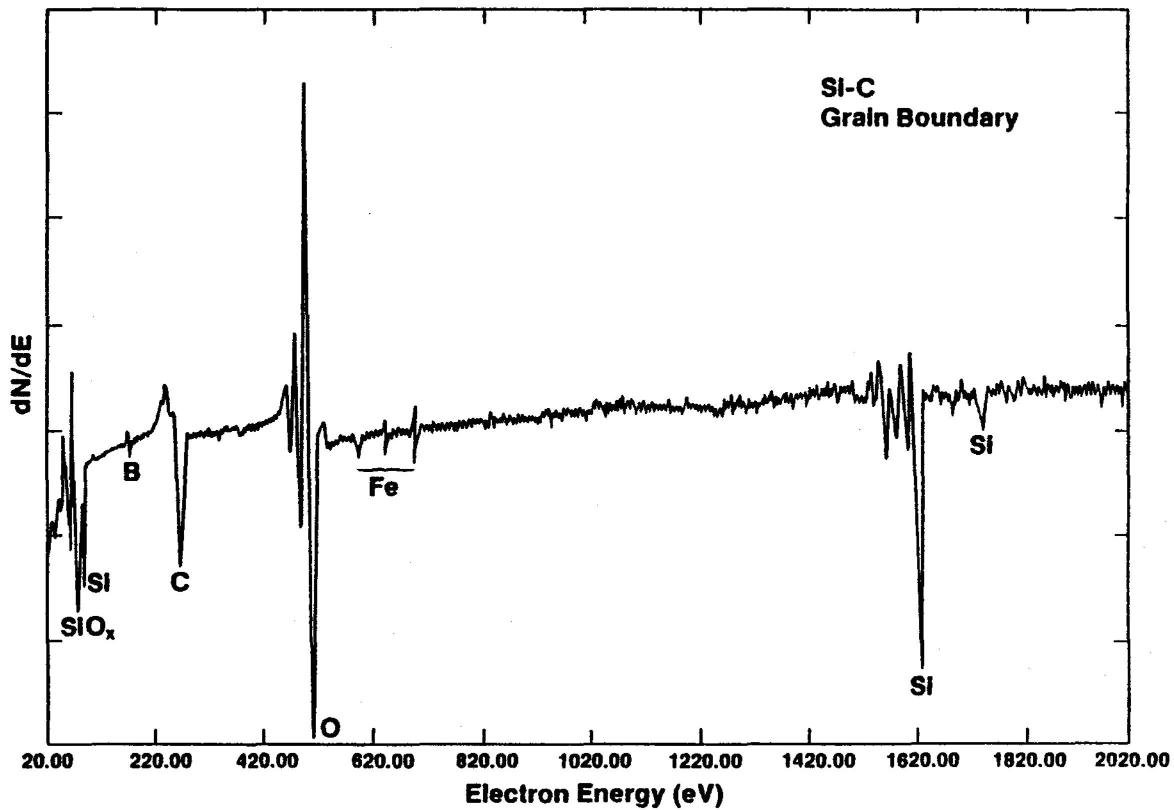

(b)

Fig. 3 Auger electron spectroscopy spectra for fractured multigrained silicon, sample Si-C (a) Grain region; (b) Grain boundary. E_p = 5keV, I_p = 0.04μA.

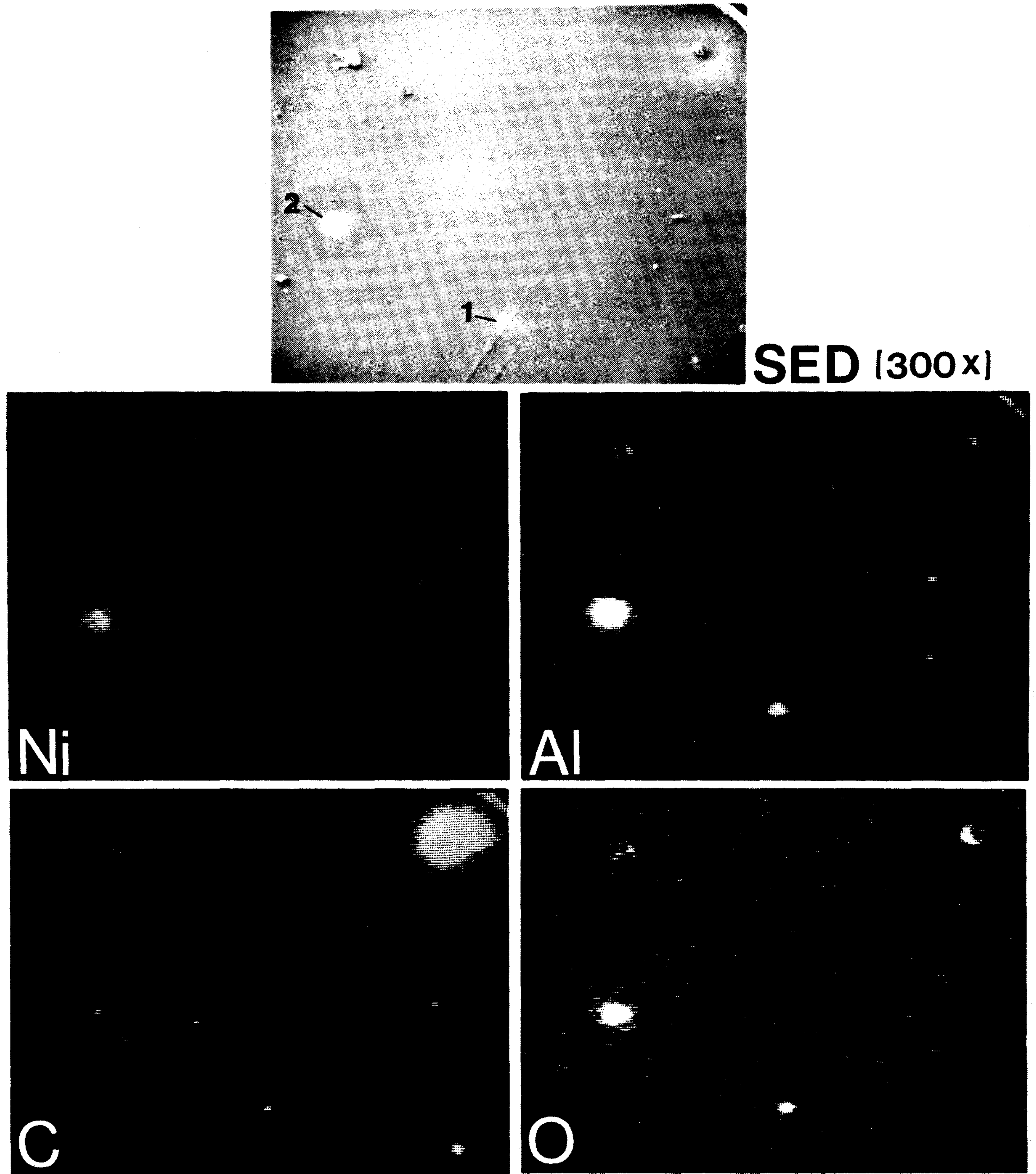

Fig. 4 Scanning Auger mapping sequence for grain boundary region. Secondary electron detection (SED) micrograph of region with Ni, Al, C and O Auger maps are presented. (Sample Si-A).

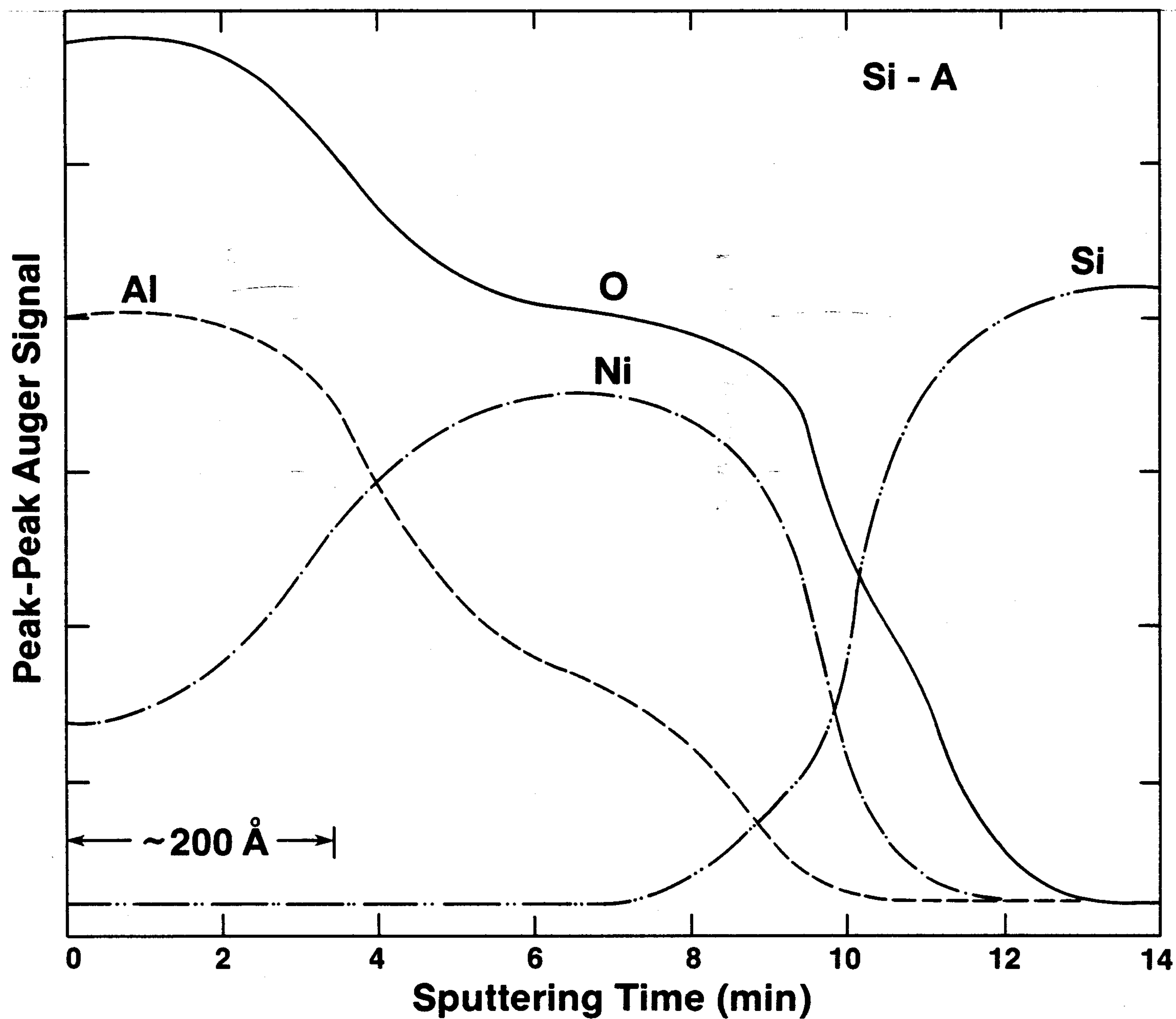

Fig. 5 Depth compositional profile of area 2 from Fig. 4 indicating localization of Ni, Al and O at grain boundary.

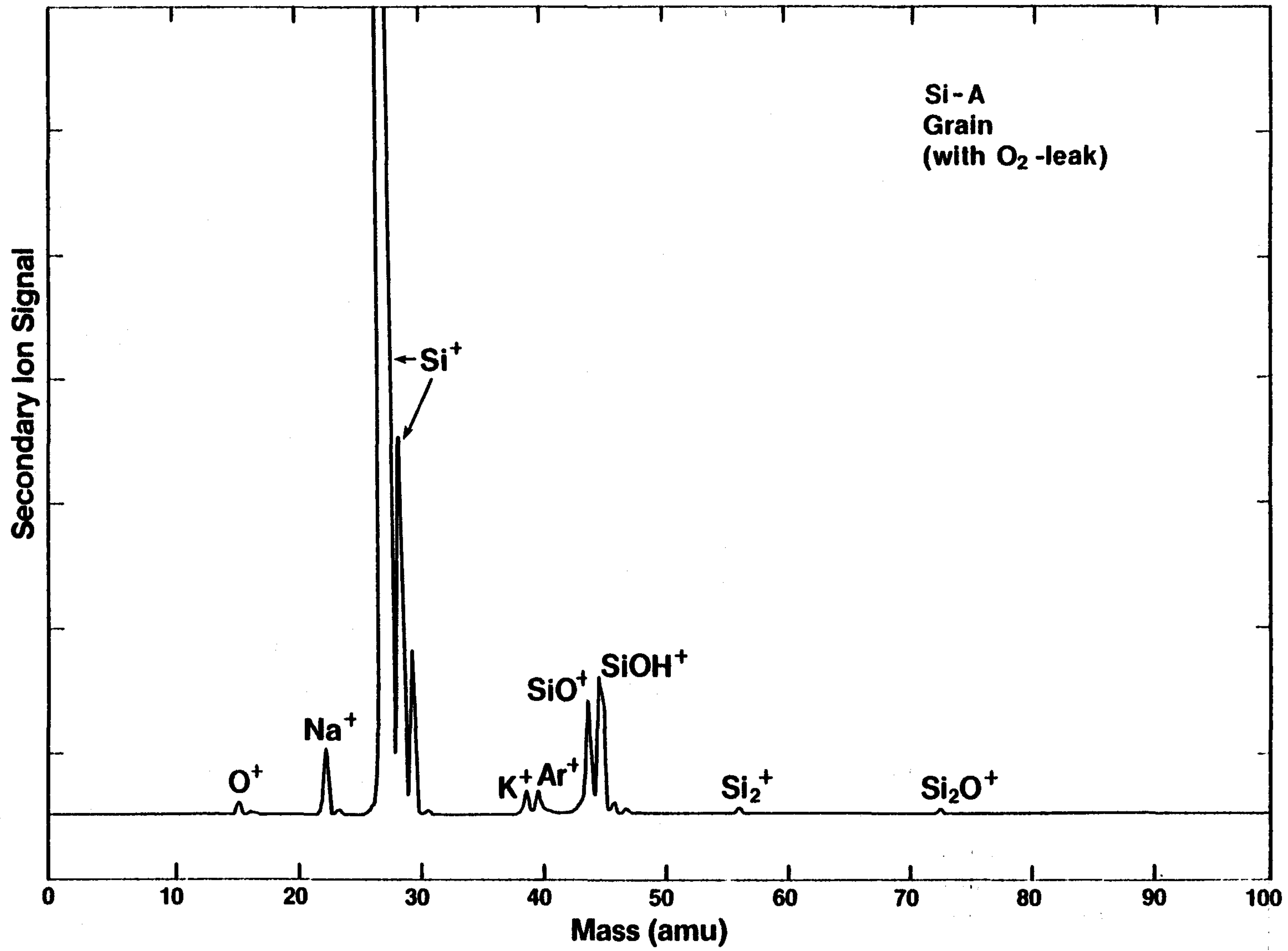

Fig. 6 Positive SIMS spectrum of fractured grain (sample Si-A), same area as shown in Fig. 3. Primary ion energy = 5kV, I_p = 260 nA, Pass energy = 25 eV, 30% gating.

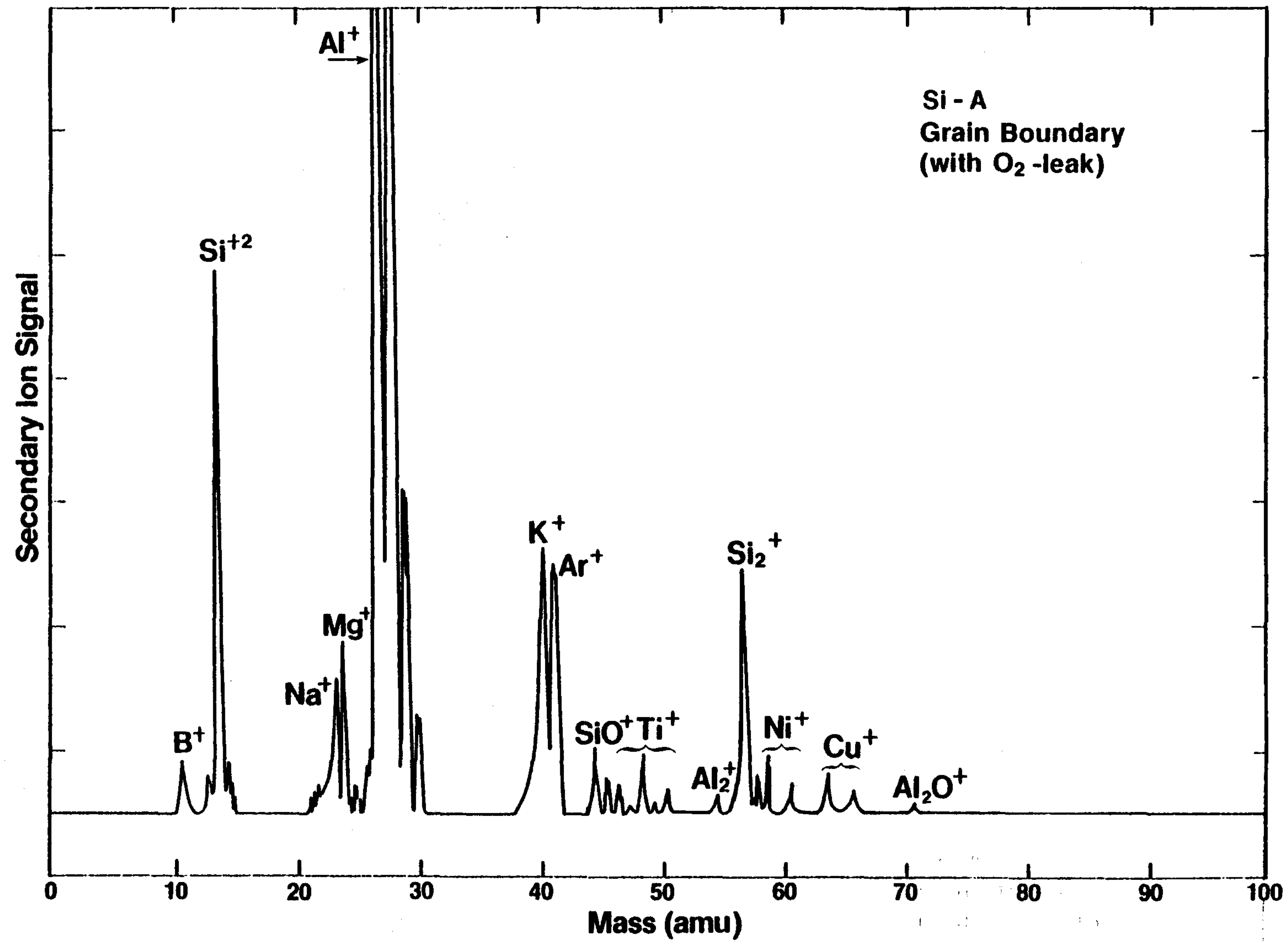

Fig. 7 Positive SIMS spectrum of grain boundary (Sample Si-A), same area shown in Fig. 3 and same conditions as in Fig. 6.

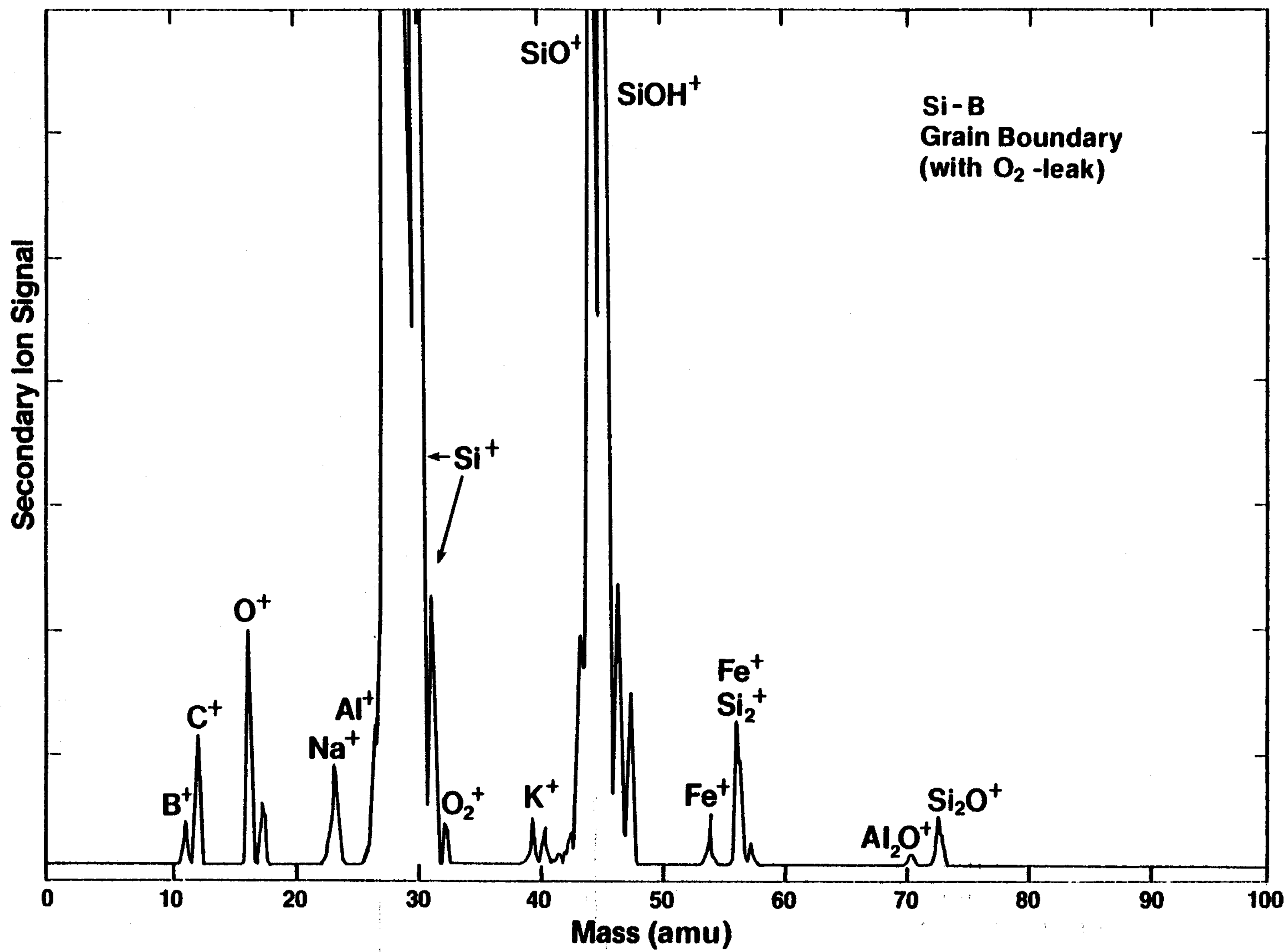

Fig. 8 Positive SIMS spectrum of grain boundary (Sample Si-B), under same conditions as Fig. 6.

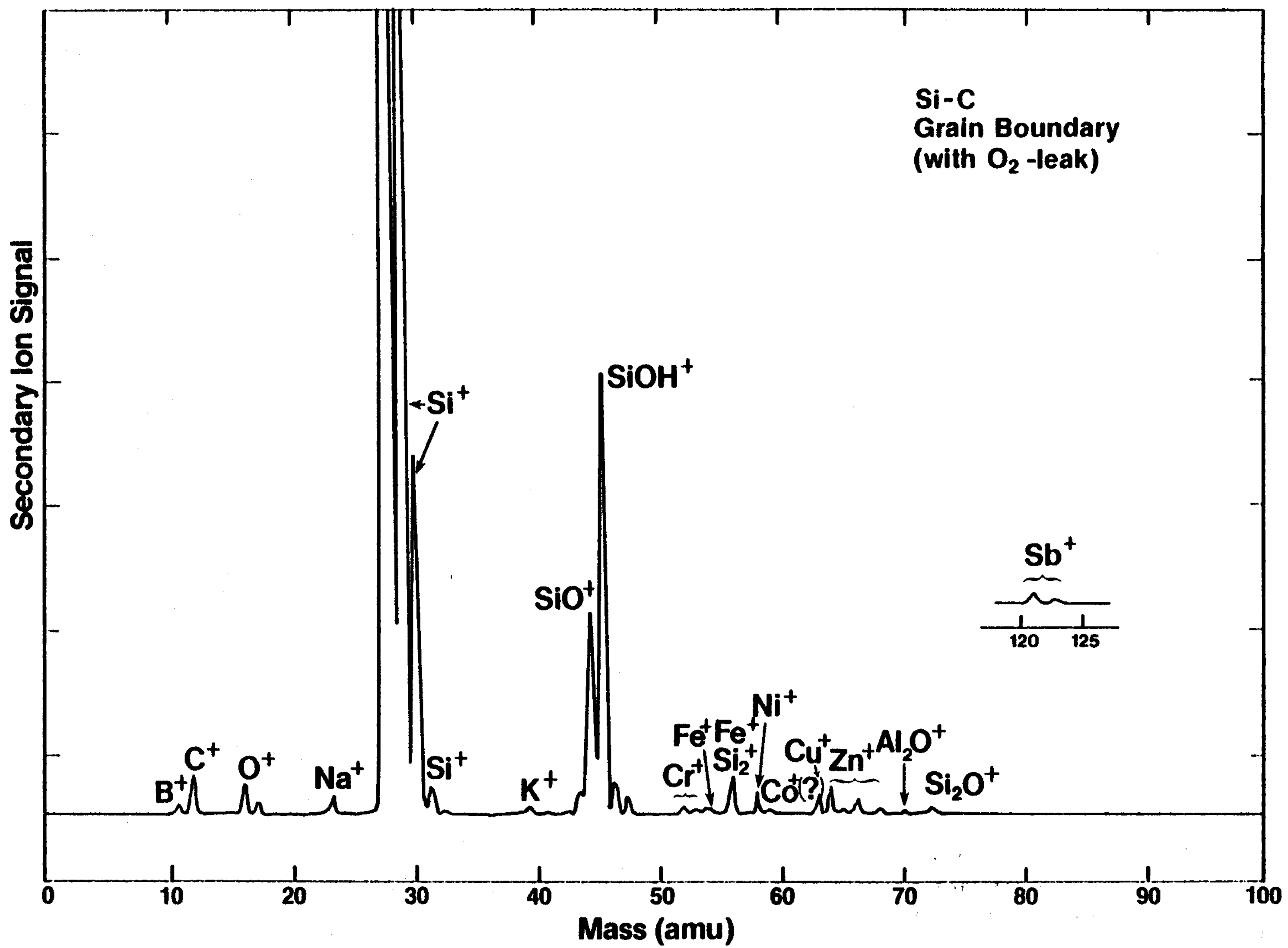

Fig. 9 Positive SIMS spectrum of grain boundary (Sample Si–C), under same conditions as Fig. 6.

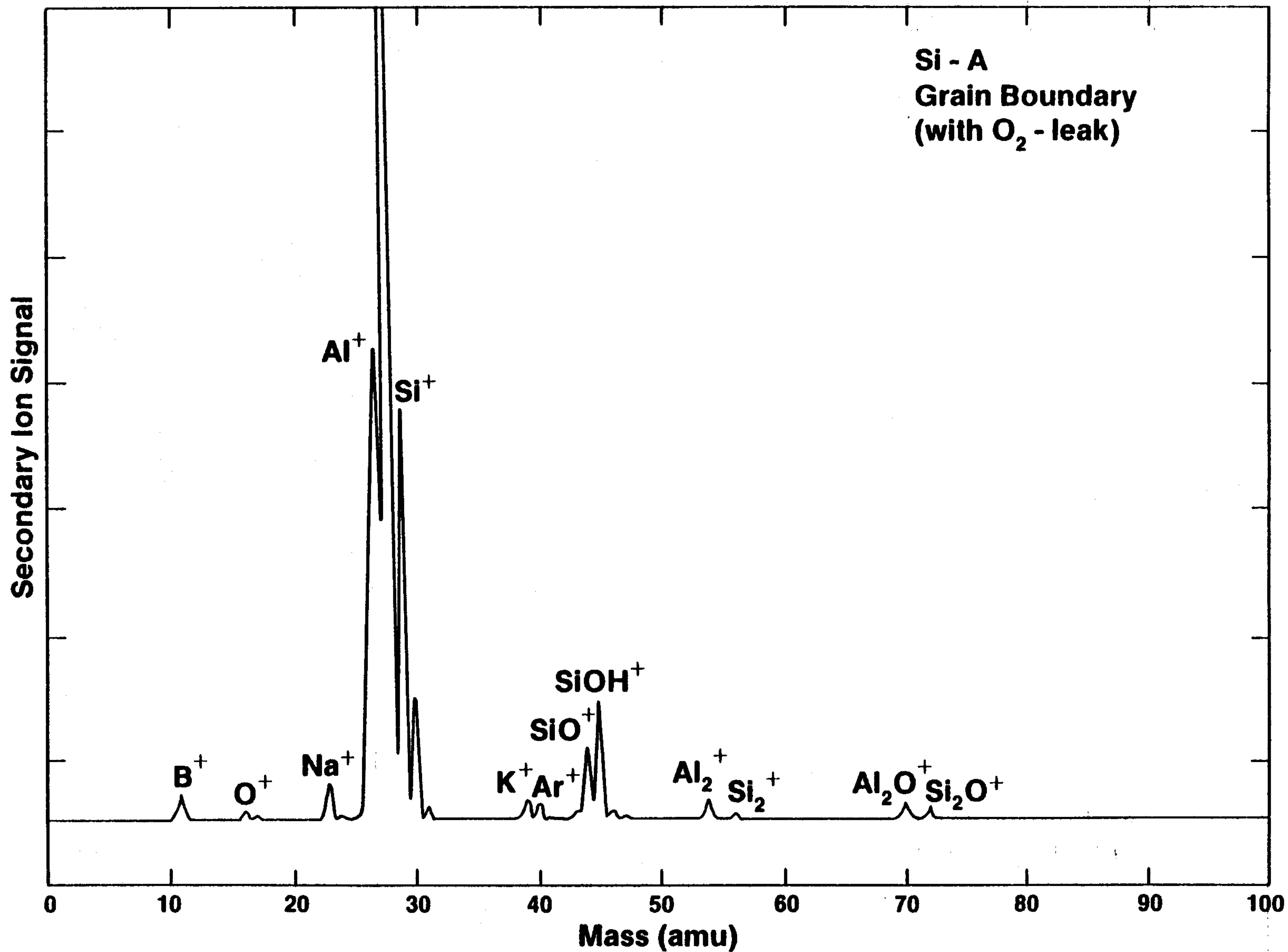

Fig. 10 Positive SIMS spectrum of a grain boundary (Sample Si-A) in the same general region as that in Fig. 7 indicating differences in impurity content. Conditions are identical to those used to generate the SIMS spectrum of Fig. 7.

DISTRIBUTION LIST

No. of Copies	Distribution
1	U.S. Department of Energy: DOE, SERI Site Office Attn: David C. Rardin, Director
1	Chicago Operations Office Interim Program Division Attn: M. E. Jackson
1	Division of Solar Technology Office of Asst. Director for Administration Attn: R. H. Annan
1	Office of Asst. Secretary for Conservation & Solar Applications Attn: F. Morse
1	Office of Solar, Geothermal, Electric & Storage Programs Attn: Martin Adams
1	Division of Energy Technology Administration Attn: S. Hansen
1	Division of Distributed Solar Technology Office of the Director Attn: R. San Martin
1	Division of Central Solar Technology Office of the Director Attn: H. Coleman
1	Division of Energy Storage Systems, ETS Office of the Director Attn: G. Pezdirtz
1	Division of Planning & Energy Transfer, ETS Office of the Director Attn: Leslie Levine
1	Wind Energy Systems Attn: L. Divone

NREL National Renewable Energy Laboratory
02LIB085768